

A model that reconciles major- and trace-element data from abyssal peridotites

Paul D. Asimow *

Lamont–Doherty Earth Observatory, Palisades, NY 10964–8000, USA

Received 4 June 1998; revised version received 30 March 1999; accepted 30 March 1999

Abstract

Abyssal peridotite samples from slow-spreading oceanic ridges have been interpreted as residues of near-fractional melting processes on the basis of trace-element data, whereas major-element compositions and modes of the same samples require interactions between migrating melts and residual solids, either by equilibrium porous flow, refertilization, or olivine crystallization. Modeling of major- and trace-element data shows that these peridotite samples are consistent with a variety of melting and melt migration histories that include elements or episodes both of near-fractional melting and of equilibrium porous flow. A component of equilibrium porous flow explains peridotite compositions better than olivine deposition or refertilization. Mixing of primary basalt liquids composed of variable proportions of unmodified liquid increments extracted by near-fractional melting, and of liquids transported by equilibrium porous flow generates local trend systematics like those observed in fractionation-corrected basalt compositions at slow-spreading ridges. Both the local trend in basalts and the fractionated trace elements in peridotites are absent at the fast-spreading East Pacific Rise, allowing simpler models of melting and melt migration than those required at Atlantic and Indian ridges and implying a spreading-rate or magma-flux dependence to the mechanism of melt extraction. © 1999 Elsevier Science B.V. All rights reserved.

Keywords: peridotites; mid-ocean ridge basalts; mantle; partial melting; segregation

1. Introduction

Basalt and peridotite samples recovered from mid-ocean ridges represent the complementary liquid and residual products of melting and melt migration processes in upwelling oceanic mantle. Chemical data from these rocks provide the essential evidence that constrains the nature of these processes; in particular, whether melting is near-fractional (i.e., a system from which melts are continuously removed

and chemically isolated from residues, perhaps with a small residual porosity remaining behind), or whether there is significant equilibration between liquids and residues after the liquids are formed (either in situ or along melt migration pathways). Several lines of evidence have led to widespread acceptance of the role of near-fractional melting in the production of the igneous oceanic crust at mid-ocean spreading centers, but none of these arguments is definitive.

First, textural evidence that basaltic liquids are interconnected at low melt fraction [1,2], together with physical arguments concerning compaction and

* Tel.: +1-914-365-8712; Fax: +1-914-365-8155; E-mail: asimow@ldeo.columbia.edu

porous flow [3] and measurements of disequilibrium in the daughter isotopes of ^{238}U and ^{235}U in fresh basalts [4,5] imply that liquids can and do become mobile at small porosities and are rapidly extracted from the mantle [6–8]. Low residual porosity, however, does not directly imply fractional or even near-fractional melting, despite the intuitive relationship between these phenomena. In principle, melts migrating by porous flow can remain in equilibrium with the solid matrix whatever the porosity. Indeed, equilibrium porous flow models utilizing very low residual porosity can explain the U-series disequilibrium data [9,10], and may be required to explain correlations between U-series disequilibria and other measurements [11]. The extent of equilibration expected in porous flow models depends on the spacing of channels [12,13] rather than the porosity per se. In one dimension and steady state, the limit of perfect equilibrium between migrating melts and matrix in fact yields liquid and residue compositions identical to batch, rather than fractional, melting, regardless of porosity [10,14,15]. Furthermore, the existence of replacive dunite bodies in the mantle sections of ophiolite exposures is generally taken as evidence that melts migrating by porous flow do in fact react with the matrix at least within high-flux channels [16–19], and the same process may be operating on harzburgites as well [20].

Second, the forward model of aggregate basalt production of Langmuir et al. [21] obtains a better fit to regionally averaged, fractionation-corrected mid-ocean ridge basalt (MORB) compositions using a fractional melting process than a batch melting process. The fractional melting model of Langmuir et al. [21] provides, however, such a small range in the Fe contents of primary liquids in a melting regime of given potential temperature that it is not possible to explain the slow-spreading local trend of Klein and Langmuir [22] by melting processes even with complete freedom to imagine arbitrary mixing scenarios. The batch melting model of Langmuir et al. [21] (which does not fit the global trend well) does provide enough range in Fe to create these local trends, given a suitable rule for generating a range of partial mixtures of primary liquid increments.

Third, trace-element data from clinopyroxene (cpx) grains in abyssal peridotites recovered from the slow-spreading Indian and Atlantic ridges pro-

vide the most convincing evidence for near-fractional melting with residual porosity in the range 0.1–1% [23,24]. Nearly all the interpretations of abyssal peridotite (and basalt) data to date have used models wherein the mode of melt extraction and/or the porosity are constant. This is certainly a reasonable first approach, since it is inherently simpler than any variable-mechanism or variable-porosity model. Under the constraint of constant mechanism and porosity, it is indeed difficult to explain the trace-element data of [23,24] except by low-porosity near-fractional melting. As we will see below, however, no simple one-stage model with constant parameters can simultaneously explain both the trace-element and major-element systematics of abyssal peridotite. Reluctantly, then, we must expand our parameter space to include more complex models. For trace elements, this point has been made by Kelemen et al. [19], who observed that the REE patterns in cpx of Johnson et al. [24] are consistent with combinations of batch and fractional melting in addition to constant porosity near-fractional models.

The behavior of major elements in peridotites and of basalt compositions during combined histories of equilibrium transport and fractional melting has not previously been described. In this paper I show that elements of both equilibrium transport and near-fractional melting are required to explain major-element trends in abyssal peridotites, and that such combinations are consistent with trace-element and modal data from peridotites as well as major-element data from MORB. The coexistence of differing styles of melting or of a continuum of melting styles in the same melting regime is a natural consequence of reasonable physical scenarios of melt migration and accounts for enigmatic aspects of diverse data types.

2. Abyssal peridotites

The major-element data for slow-spreading ridges consist of (1) 36 distinct plagioclase-free lherzolite or harzburgite samples from the southwest Indian ridge [23,25] with published primary mineral modes and analyses of relicts of all phases, allowing direct estimation of the bulk composition; (2) 86 further samples from Indian and Atlantic ridges, for which primary mineral modes and between zero and three

mineral analyses were published [23–25] and bulk compositions have been estimated using correlations among phase compositions and modes by Niu et al. [26] and Niu [27]. I have attempted to reproduce the reconstruction method of Niu et al. [26] and found apparent discrepancies in sample selection, Cr₂O₃ contents, and TiO₂ contents, and an ambiguity leading to at least two different possible results for FeO. In what follows I use my own results (following, where possible, the method of Niu et al. [26]) rather than the published reconstructions of Niu et al. [26]; the FeO contents used here are consistent with earlier unpublished versions of the Niu et al. method (C. Langmuir, pers. commun.), with the alternative reconstruction of Baker and Beckett [28], and, a posteriori, with the modeling results presented. Given the substantial uncertainty in reconstruction, the reader may choose to evaluate the petrogenesis of abyssal peridotites solely from those samples where all phases have been analyzed (shown as filled symbols in all the figures herein).

Ion-probe trace-element data (Ti, Zr, and REE) from cpx grains are available for two of the fully analyzed samples and 39 of the reconstructed samples [23,24]. For the fast-spreading East Pacific Rise, complete modes and major-element analyses have been reported only for 9 harzburgites drilled from Hess Deep, among which 5 samples have reported cpx trace-element analyses [29].

2.1. Fractional melting

Quantitative modeling of the major-element evolution of melting residues was first attempted by Niu et al. [26] and Niu [27], who concluded that abyssal peridotites are not residues of fractional melting (or of isobaric batch melting), using the parameterized mantle melting models of Niu and Batiza [30], Kinzler [31], and Langmuir et al. [21]. This conclusion does not depend on which version of the Niu et al. [26] reconstruction is used. I confirm their result using a thermodynamically self-consistent, incrementally isentropic fractional fusion calculation based on the MELTS model [32–35]. Fig. 1 plots oxides against MgO for abyssal peridotite samples and MELTS calculations of residues of polybaric fractional fusion using various potential temperatures, with melting continuing to the base of the crust.

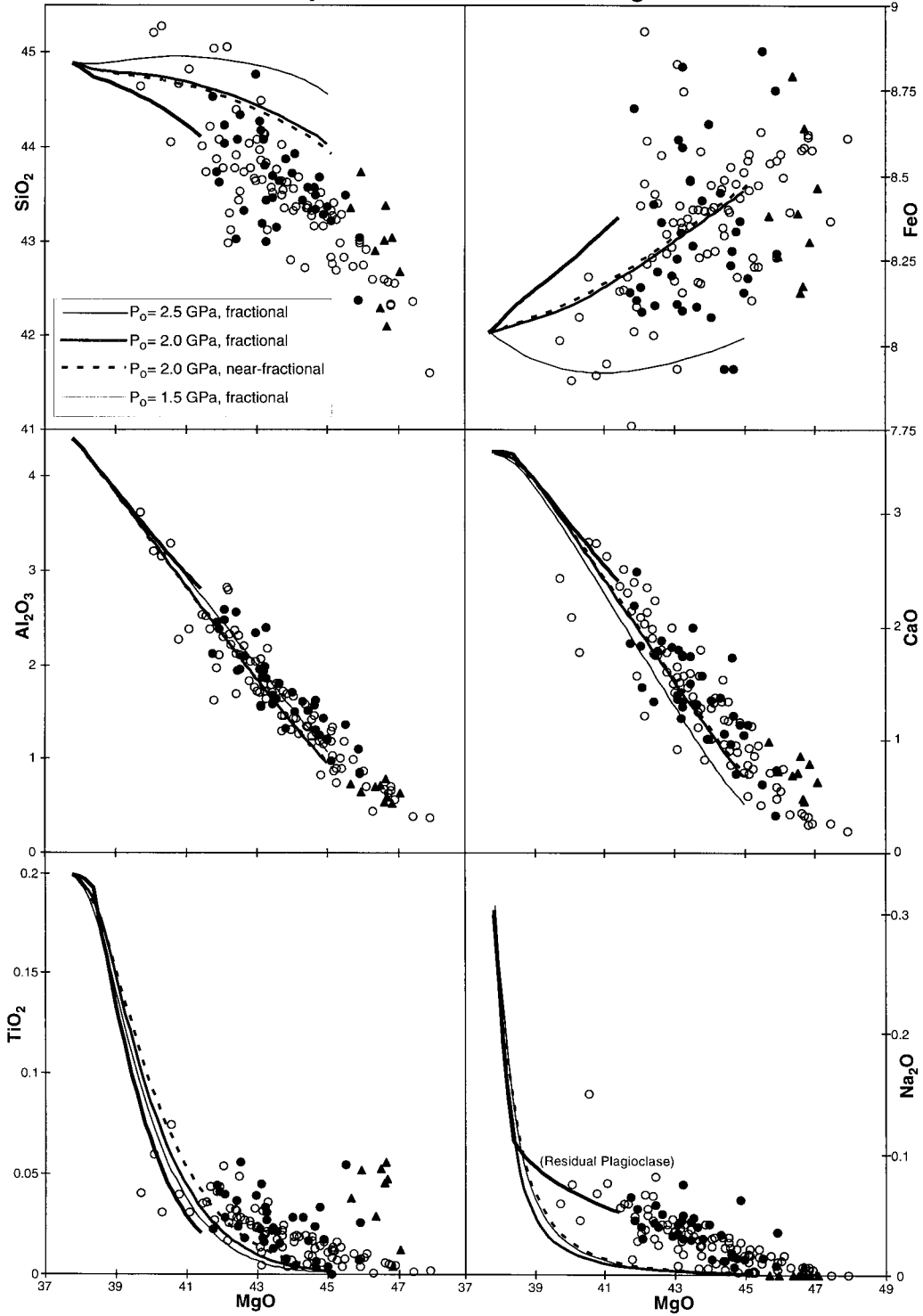
I also show one near-fractional melting calculation with a residual porosity of 1%; it is effectively identical to perfect fractional melting in major oxides. These calculations grossly fail to reproduce the low SiO₂, high FeO end of the trend, and give TiO₂ and Na₂O much too low and CaO perhaps slightly too low at a given MgO content. None of these calculations reaches high enough MgO content to explain the most refractory samples; using higher potential temperatures to reach higher extents of melting and higher MgO exacerbates the FeO and SiO₂ problems by increasing the mean pressure of melting. Refertilization of fractional residues with basalt [36] would not help explain the high MgO or low SiO₂ samples. These results are essentially similar to those of Niu et al. [26], except that fractional fusion with MELTS along adiabats that intersect the solidus at less than 2 GPa gives a positive slope in the FeO–MgO diagram comparable to the trend of the abyssal peridotite data, failing only to reach the most Fe–Mg-rich samples, whereas the models plotted by Niu et al. [26] yield nearly horizontal FeO–MgO paths able to explain only the most Fe–Mg-poor samples.

2.2. Polybaric batch melting or equilibrium transport

As an alternative to the fractional or near-fractional model, consider isentropic polybaric batch melting. Fig. 2 compares the abyssal peridotite samples to MELTS calculations of isentropic batch melting at the same potential temperatures as Fig. 1. Given the range of possible source compositions and potential temperatures, this process appears to produce an excellent fit for all oxides, except Na₂O (the data are too high in Na₂O at given MgO) and TiO₂ (much of the data are too low at given MgO). Polybaric batch melting is able to produce nearly opx-free samples with up to 49% MgO if melting continues to very low pressure (~0.2 GPa). Given that batch melting of peridotite with MELTS as currently calibrated is known to produce liquids higher in SiO₂ and Na₂O and lower in MgO than 1 GPa experiments [37,38], the residues calculated from MELTS presumably err somewhat towards high SiO₂ and low Na₂O at given MgO.

In steady state and one dimension, polybaric batch melting produces residues identical to those

Polybaric Fractional Melting



generated by equilibrium porous flow [15], so in general terms the formation of high-MgO residues approaching and including dunite in these calculations is equivalent to the models for dunite formation by reactive porous flow discussed by Kelemen and coworkers [16,18–20], although these authors envision formation of dunite at pressures near 1 GPa. Abyssal harzburgites look like products of the same process that makes ophiolite dunites, but the process has not gone to completion. The melt focusing calculations of Asimow and Stolper [15] show that there is a wide range of focusing factors and potential temperatures where focused equilibrium porous flow leaves a harzburgite residue; such harzburgites are distinguishable from fractional residues not only by their trace-element patterns but also by low SiO₂ and high FeO, CaO, and TiO₂ at given MgO.

The misfit for Na₂O is curious; not only are the estimated bulk Na₂O contents of Atlantic and Indian Ocean abyssal peridotites too high at given MgO to be residues of near-fractional melting, they are higher even than expected from polybaric batch melting [36]. Trace elements with partition coefficients similar to that for Na, on the other hand, show concentrations in cpx significantly lower and ratios significantly more fractionated than can be produced by batch melting models [24]. Part of the misfit seen in Fig. 2 is due to the underestimate of the partition coefficient for Na₂O in the current MELTS calibration [38], but it seems likely that the bulk Na contents of abyssal peridotites have not been well characterized. Many published electron probe measurements of Na in abyssal peridotites may be upper limits (H.J.B. Dick, pers. commun.). The drilled Hess Deep samples have significantly less Na than equally depleted dredged samples from other locations, and samples from the Teravaka transform on the East Pacific

Rise (and elsewhere; Baker and Beckett, submitted) clearly have a bimodal distribution of Na contents in cpx grains [39]. Unless bulk Na₂O concentrations are attributed to analytical problems or metasomatism, Na will remain a problem in this analysis.

Baker and Beckett [28] calculate an alternative reconstruction of 43 site-averaged abyssal peridotite bulk compositions based on the raw data of Dick and coworkers and Bonatti and coworkers [23,29,40–43], leading to bulk composition trends similar to those of Niu et al. [26], except for FeO vs. MgO (Fig. 3). Baker and Beckett attribute the positive correlation between FeO and MgO in the Niu et al. reconstruction partly to the use of individual thin sections, which may be too small to accurately characterize their modes, rather than site averages. By analogy to basalt compositions, however, where regional averages are thought to reflect long-wavelength variations in potential temperature [44], and individual samples are thought to reflect processes within the melting regime at fixed potential temperature [22], it is possible that site averages of abyssal peridotite compositions may also reflect a more global systematic than individual thin sections (in addition to any effects of point counting statistics). In Fig. 2 each polybaric batch melting model curve represents progress up a single column with given potential temperature, which produces a curve resembling the trend of the unaveraged abyssal peridotite compositions from the method of Niu et al. [26]. On the other hand, Fig. 3 superimposes selected global vectors, obtained from columns over a range of potential temperatures. The long-dashed curve samples each potential temperature at equal pressure (0.3 GPa), and gives higher FeO at low potential temperature and moderate MgO than the bulk of the Baker and Beckett site averages. A global trend drawn at the

Fig. 1. Comparison of residues of incrementally isentropic polybaric fractional melting calculated using MELTS to bulk compositions of abyssal peridotites (all axes are weight percent oxides). Filled circles indicate samples from Atlantic and Indian Ocean ridges for which modes and analyses of all phases are available allowing direct estimation of bulk composition [23,25]. Open circles indicate samples from Atlantic and Indian Ocean ridges for which bulk compositions are reconstructed by a method similar to that of Niu et al. [26] using modes and analyses of zero to three phases [23–25]. Filled triangles are (fully analyzed) samples from Hess Deep in the Pacific Ocean [29]. Calculations use the primitive mantle source composition of McDonough and Sun [57]. The method of calculation is as described in [34]; all liquid is extracted from the system each time an increment of 0.5% by volume is generated by isentropic upwelling (except for the short-dashed black curves, which show a near-fractional calculation with residual porosity of 1.0%). Only the lowest potential temperature path experiences residual plagioclase at low pressure; other paths are too depleted by the time they reach the stability field of plagioclase.

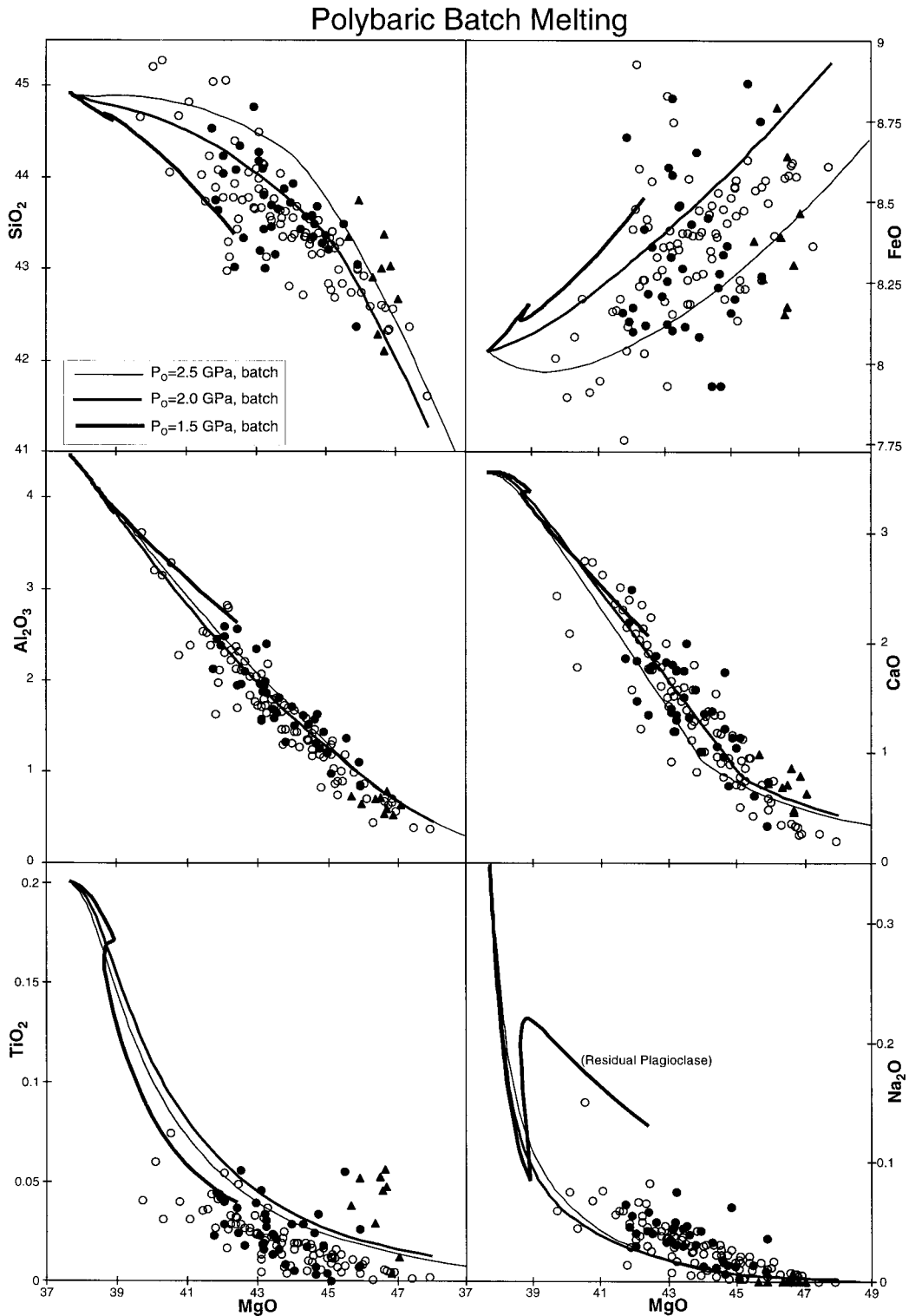


Fig. 2. Comparison of residues of isentropic polybaric batch melting calculated using MELTS to bulk compositions of abyssal peridotites. Symbols and data sources as in Fig. 1.

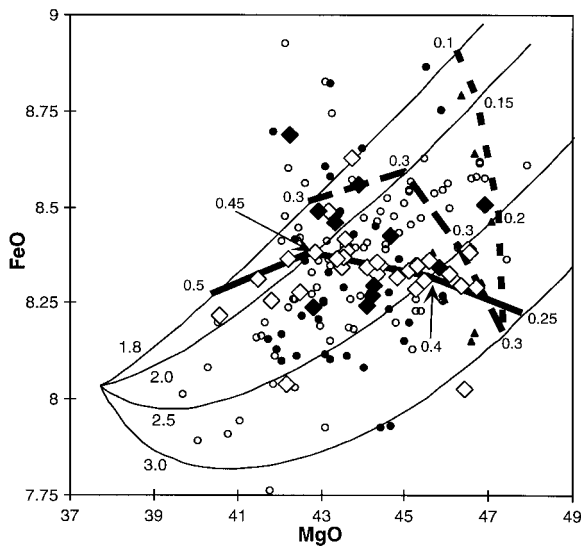


Fig. 3. Comparison of total FeO vs. MgO for site-averaged abyssal peridotite compositions and individual abyssal peridotite thin sections. Small circles and triangles are the same data as shown in Figs. 1 and 2. Large diamonds show the site averages obtained by Baker and Beckett [28]; filled for suites where all phases have been analyzed and open for suites where bulk composition has been reconstructed despite unmeasured phases by a somewhat different method than that of Niu et al. [26]. Fine curves are isentropic polybaric batch melting curves for the McDonough and Sun bulk silicate earth source [57] at four different potential temperatures, labeled by the pressure (in GPa) where the adiabat intersects the solidus. Heavy curves show 'global trends' obtained by connecting residue compositions from different potential temperatures; the pressures where the black and shaded curves intersect are marked in GPa. The long-dashed curve shows constant pressure (0.3 GPa). The short dashed curve is for simple two-dimensional melting regimes where melting continues to the base of the crust and abyssal peridotites are sampled at the pressure of the base of the crust. The solid black curve is chosen to fit the Baker and Beckett data and implies sampling of low-potential temperature regions at higher pressure (0.5 GPa) and high-potential temperature regions at lower pressure (0.25 GPa in this case).

pressure of the average base of the crust for each potential temperature yields the steep short-dashed curve in Fig. 3, a worse fit to the Baker and Beckett data. To get a flat or gently-sloping global trend requires sampling at higher pressure where potential temperature is low, and lower pressure where potential temperature is high (solid black curve in Fig. 3; pressures are picked to fit), the opposite of control by crustal thickness. The site-averaged abyssal peridotite data perhaps therefore imply that

the thermal structure at fracture zones is affected by the temperature of the underlying mantle, with a thinner lithosphere at fracture zones overlying hot mantle (which could also be a spreading-rate effect, since most low potential temperature regions have slow spreading rates). This inferred thermal structure is consistent with the inference of Michael and Cornell [45] that fractionation of basalts occurs at higher pressure along cold or slow-spreading ridge segments than along hot or fast-spreading ridge segments.

2.3. Combinations of fractional melting and equilibrium transport

The observation that abyssal peridotites resemble residues of polybaric batch melting in major-element composition is interesting but unsatisfying, because:

- (1) trace elements in cpx suggest some near-fractional melting in the Atlantic and Indian samples [23,24];
- (2) the global trend in basalt composition is more consistent with fractional melting [21];
- (3) batch melting strictly speaking is physically unlikely since melts are presumed to be mobile; and
- (4) primitive MORB liquids are far from equilibrium with orthopyroxene (opx) at pressures less than about 1 GPa [46] and hence much of the liquid presumably migrates through the shallow mantle in isolation from opx [18]. This implies that we ought to test the consequences of histories that combine batch and fractional melting as a preliminary description of histories in which the residual porosity, melt flux, and/or extent of equilibration along flow paths vary during upwelling. Our goal is to find hybrid models that can explain both major- and trace-element compositions of abyssal peridotites and basalts in a manner consistent with physical constraints on melt transport.

As an example of the potential of models with varying melting mechanisms, consider the cases of fractional melting followed by a switch to batch melting and, conversely, batch followed by fractional melting. These are intended to describe melting regimes like those envisioned by Hart [13] with a fractal network of high-porosity channels. There is some finite porosity everywhere, but instead of uniform porous flow without horizontal structure, we

consider that the flow tends to break up into regions of relatively high porosity and melt flux (generically labeled channels without consideration here of their formation mechanism; proposals include [47–49]) and complementary regions of relatively low porosity and melt flux. Outside a channel the system is undergoing a process close to near-fractional melting in that liquids are removed as they are formed but very little is added to the system, whereas inside a channel melts are fluxing through and re-equilibrating to some extent with the residue in the channel. In the solid frame of reference, the essential control on the character of melting is not melt velocity but rather how much melt enters from below and whether it is allowed to interact with the local solid. Here the interior of the channels is modeled using perfect equilibrium because kinetic partial-equilibrium models for major elements are not available; by combining episodes of the end-member processes of fractional and equilibrium flow we attempt an approximate description of a system which experiences a range of intermediate behavior.

The number of channels may increase or decrease upwards due to the competition between coalescence of channels and nucleation of new channels. The melt flux carried by channels, however, certainly increases upward due to progressive melting and increases laterally towards the ridge axis due to melt focusing. Probably, therefore, the volume fraction of channels ought to increase upwards and towards the ridge axis. In a parcel of mantle that reaches shallow levels near the ridge axis and can be sampled as abyssal peridotite, then, the sequence fractional-followed-by-batch should be most common, but in real melting regimes the channels may be mobile and a given sample may switch modes several times or experience a random-walk in porosity.

In Fig. 4, the residues of MELTS calculations of varying extents of fractional melting followed by batch melting, and of varying extents of batch melting followed by fractional melting (with all calculations continuing to the base of the crust), are compared to abyssal peridotite samples. Clearly, it is difficult to distinguish these combined histories from simple polybaric batch melting paths in oxide vs. MgO space, although a component of fractional melting helps to explain the TiO₂ data. The data appear to permit any of these histories (again, with the

exception of Na₂O). This calculation, then, is similar to the result of Kelemen et al. [19] for REE patterns: the major- and trace-element data from slow-spreading ridges are consistent with combined histories of batch and fractional melting, and it is difficult to distinguish the order or relative amounts of each. The difficulty comes in part from the weak effect of near-fractional melting on major-element evolution and the weak effect of batch melting on trace-element composition. Similarly, the Ti–Zr plot, that Johnson et al. [24] used to argue that abyssal peridotites are residues of various degrees of near-fractional melting, is equally consistent with combinations of batch and fractional melting.

In the fractional-then-batch model the small melt fraction liquids that are extracted during the early fractional melting episode do not interact with overlying mantle during ascent. The trace-element constraints from abyssal peridotite are satisfied by removing the enriched early melts carrying high concentrations of incompatible elements from that part of the system that reacts to form abyssal harzburgites. Perhaps the early melts are transported in dunite conduits [16] as observed in ophiolites, but not included in the population of abyssal harzburgites considered here.

The fractional-then-batch model can satisfy the constraint that primitive aggregate MORB is undersaturated in opx at low pressure [46] in a number of ways. First, the fractionally transported component may constitute the bulk of the aggregate liquid since, coming from the wide base of the triangular melting regime, it is disproportionately weighted in the integrated composition [50]. Second, the calculations in Fig. 4 only consider one-dimensional (vertical) melt transport. In the usual description of a two-dimensional batch-melting regime, liquid that undergoes equilibrium transport through the melting regime but reaches the boundary of the melting regime off-axis at depth, is subsequently transported to the crust without further reaction (in the present hybrid model, perhaps in the same dunite channels that are carrying fractional liquids from still deeper). Third, many of the equilibrium transport conduits may collect sufficient melt flux to generate dunite near 1 GPa and subsequently transport liquids in isolation from opx [15,16]. Formation of dunite by equilibrium porous flow at 1 GPa requires focusing

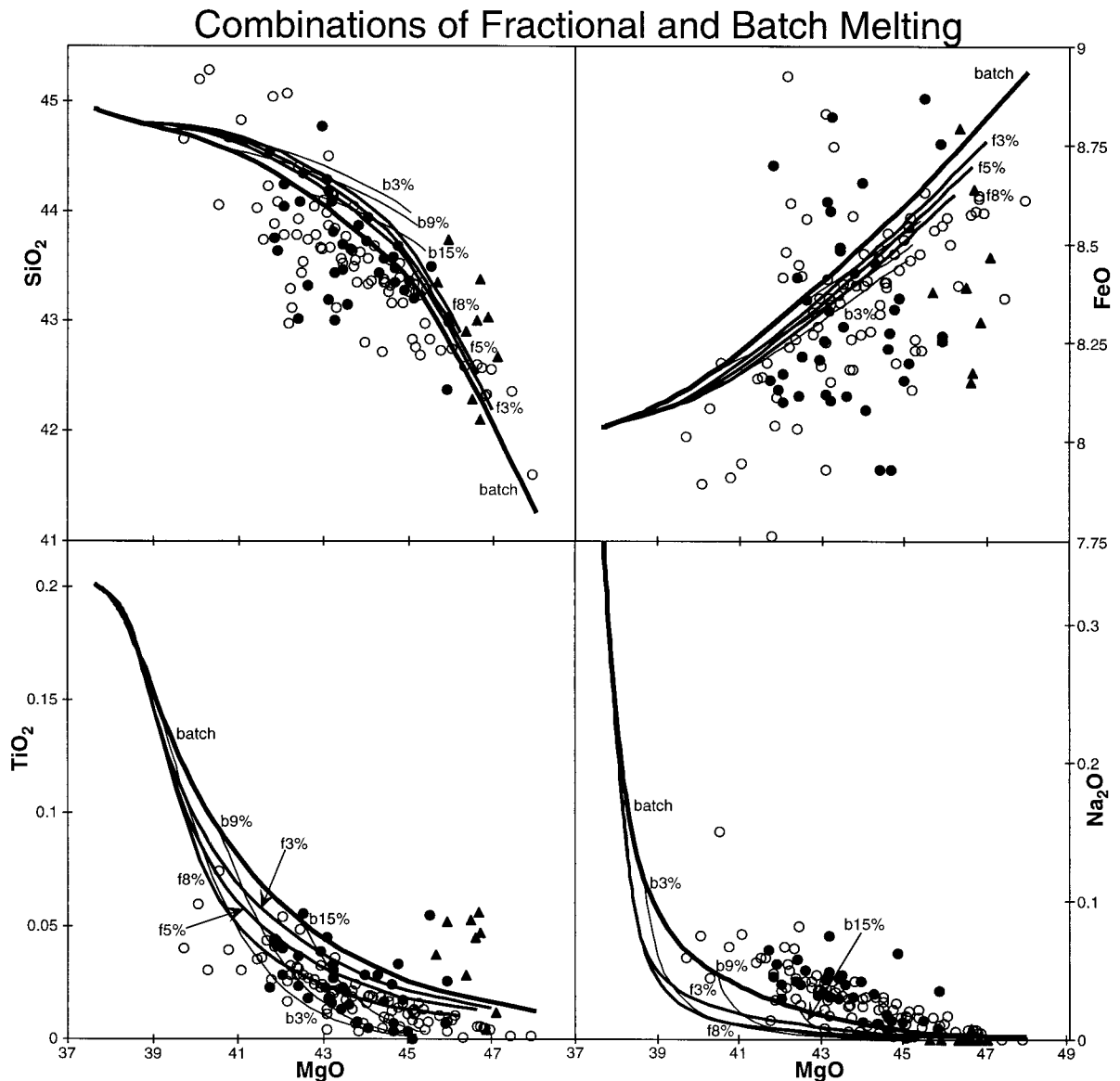


Fig. 4. Comparison of residues of combinations of polybaric fractional and batch melting using MELTS with bulk compositions of abyssal peridotites. Symbols and data sources as in Fig. 1. For clarity, the potential temperature such that the adiabat intersects the solidus at 2 GPa, is shown. The curves represent batch melting (3-point curve thickness) as in Fig. 2; some fractional melting followed by batch melting to the base of the crust (2-point curve thickness, labeled with an 'f' and the extent of fractional melting used, e.g., f5% represents 5% fractional melting followed by batch melting); and some batch melting followed by fractional melting to the base of the crust (1-point curve thickness, labeled with a 'b' and the extent of batch melting used). CaO and Al₂O₃ are not shown as all curves overlap the batch melting curve.

the melt flux; diffuse flow involving the entire mass of residue is not sufficient to generate dunite, even at low pressure [15]. The failure of the near-fractional model (Fig. 2) to produce harzburgites with

abyssal peridotite compositions, however, shows that not all of the melt flux is carried in dunite conduits. There must be a component of reactive vertical flow leaving modified harzburgite residues that can be

sampled as abyssal peridotite, and this reaction must continue to pressures significantly lower (0.2–0.5 GPa, see Fig. 3) than the pressure of opx saturation in primitive MORB (~1.0 GPa). The two-layer models described here are intended only as preliminary descriptions that can simulate histories of particular hand samples of residue; clearly a model incorporating horizontal variations in the style of melt transport is necessary to satisfy all the constraints on peridotite and basalt composition.

2.4. Comparison to the olivine-addition model

A two-stage model of fractional fusion followed by olivine addition from fractional crystallization of basaltic liquids migrating through the thermal boundary layer [26,27] also explains the major- and trace-element data in abyssal peridotites for the most part, since the samples do plot in major-oxide space between fractional residues and olivine and by fiat the olivine-addition process does not affect trace elements in cpx. The viability of the olivine-addition model can be questioned on physical grounds (it is unclear how olivine addition occurs on thin-section scale without equilibration of trace elements in pyroxene [12] and how the melt remains undersaturated in opx while depositing olivine in harzburgites [51]), but it is nevertheless of interest to test the chemical implications of the olivine-addition model. In principle, near-fractional melting followed by olivine addition can be distinguished from models involving equilibrium porous flow by examining ratios, such as $\text{CaO}/\text{Al}_2\text{O}_3$, $\text{TiO}_2/\text{Al}_2\text{O}_3$, $\text{Cr}_2\text{O}_3/\text{Al}_2\text{O}_3$, Ti/Zr in cpx, and modal cpx/opx, which are sensitive to the melting process but unaffected by simple olivine addition (except perhaps at Hess Deep, which may have high Ti in olivine). The uncertainty on ratios of bulk oxides, however, is very large (and difficult to quantify). Fig. 5 demonstrates that fractional (and near-fractional, not shown) fusion generates a very narrow range of $\text{CaO}/\text{Al}_2\text{O}_3$ and $\text{Cr}_2\text{O}_3/\text{Al}_2\text{O}_3$ ratios, except at extremely low values of $\text{TiO}_2/\text{Al}_2\text{O}_3$. The significant range in these ratios in the abyssal peridotite data is better explained by combinations of batch and fractional melting in whatever order (or by initial heterogeneity of sources or by analytical uncertainty). Using the linear relationship between MgO content of residues and extent of melting de-

rived by Niu [27], the $\text{TiO}_2/\text{Al}_2\text{O}_3$ ratios alone constrain the extent of fractional melting to <18% for all but one sample and typically to ~10% for the bulk of the data (Fig. 6a). Although the data in Fig. 6a could be explained by removal of excess olivine until the samples plotted on the fractional residue curves, most of these samples are highly depleted rocks with little or no residual cpx, implying extents of melting generally higher than 10%.

Another indicator that is sensitive to melting process, but unaffected by olivine addition, is the ratio of modal abundance of cpx to that of opx. Although the modal ratio observed in abyssal peridotite samples may be modified by subsolidus exsolution (depending on the extent of recrystallization and the method of point-counting), the change in any case is relatively minor and consistent in sense: subsolidus MELTS calculations [52] show that for rocks whose initial, high-temperature mode has a small cpx/opx ratio the effect of exsolution is to increase this ratio by only a small amount even for fully recrystallized rocks where primary and secondary cpx cannot be distinguished. The cpx/opx ratio is plotted against bulk $\text{TiO}_2/\text{Al}_2\text{O}_3$ for the abyssal peridotite data alongside fractional, batch, and combined fractional-then-batch and batch-then-fractional melting histories in Fig. 6b and against Ti/Zr ratio in cpx in Fig. 6c. The bulk of the data lie to the left of the fractional melting curves in both plots, whereas subsolidus modification of the model residues would move them to the right. The sense of known errors in modes calculated by MELTS [37,38] is to underpredict the cpx/opx ratio; so the constraint shown is robust in the sense that the correct melting reaction is likely to generate fractional melting curves further to the right. Hence, fractional residues with or without added olivine are not consistent with the modes and compositions of most abyssal peridotite samples.

Consideration of ratios of oxides and modes in abyssal peridotites appears to require more thorough chemical interaction between melt and residue than is envisioned in the olivine-addition hypothesis, perhaps episodes of equilibrium porous flow. Although the chemical data do not exclude the possibility that pervasive olivine addition may have occurred, there remains no need for olivine addition once interactions such as equilibrium porous flow are involved, and simple olivine addition without other reaction

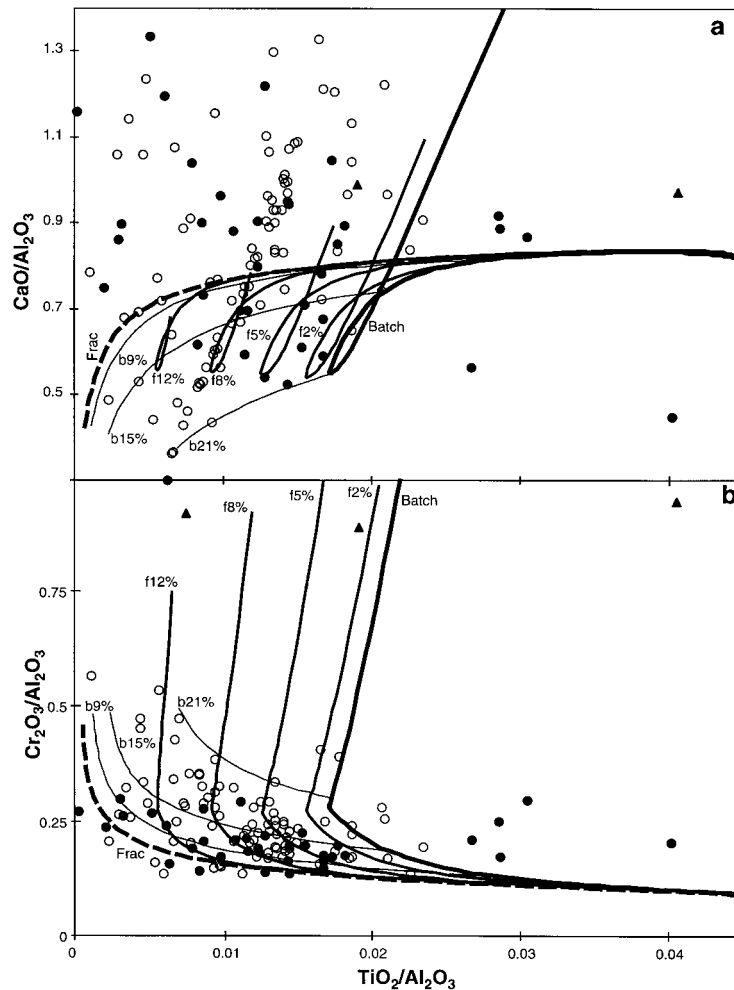


Fig. 5. Ratios of elements that should not be affected by olivine accumulation in abyssal peridotite data compared to batch, fractional, fractional-followed-by-batch, and batch-followed-by-fractional melting calculations according to MELTS. Symbols and data sources as in Fig. 1. The McDonough and Sun Bulk Silicate Earth source [57] is used with initial pressure of melting of 2.5 GPa. Curves labeled f2%, f5%, f8%, and f12% represent the labeled extent of fractional melting beginning at 2.5 GPa followed by batch melting to the base of the crust. Curves labeled b9%, b15%, and b21% represent the labeled extent of batch melting beginning at 2.5 GPa followed by fractional melting to the base of the crust.

remains physically implausible. However, the widths of the data trends in Figs. 4–6, if not the result of analytical and reconstruction errors, call for a range in source compositions (especially $\text{CaO}/\text{Al}_2\text{O}_3$) and potential temperatures as well as variation in the mechanism of melt migration.

Fig. 6 also illustrates that the harzburgite samples drilled at Hess Deep in the Pacific Ocean are anomalous compared to abyssal peridotites dredged in the Atlantic and Indian Ocean basins. Although these

rocks are extremely depleted, the Ti/Zr ratio in cpx (~ 140) is comparable to the least depleted samples from elsewhere [29]. Similarly, although the middle-to-heavy REE contents in cpx are extremely low, the overall cpx REE patterns are only moderately fractionated and the $(\text{Ce}/\text{Sm})_n$ and $(\text{Nd}/\text{Yb})_n$ ratios are higher than Atlantic and Indian Ocean samples with comparable Ce concentrations inferred to be residues of fractional melting. In Fig. 1 it is clear that all the Hess Deep samples occupy the region of

composition space that is most difficult to produce as fractional residues, whereas Fig. 2 shows that they appear consistent with polybaric batch melting or equilibrium porous flow, including Na_2O but excepting the high bulk TiO_2 contents (dominated in these samples by olivine analyses, which may be

considered analytical upper limits; H.J.B. Dick, pers. commun.). Despite their highly depleted character, these samples appear to have melted under conditions of higher porosity or more reactive flow than the Atlantic and Indian samples. Neither trace-element ratios, nor modes, nor major-element compositions (Na excepted) require a near-fractional episode in the history of these samples. The present model, however, fails to explain some aspects of the Hess Deep samples (e.g., high Ti in olivine coexisting with low Ti in cpx); a more complex history such as that described by Dick and Natland [29] may be required.

3. Basalts

An outstanding problem in the interpretation of MORB composition data is the quantitative explana-

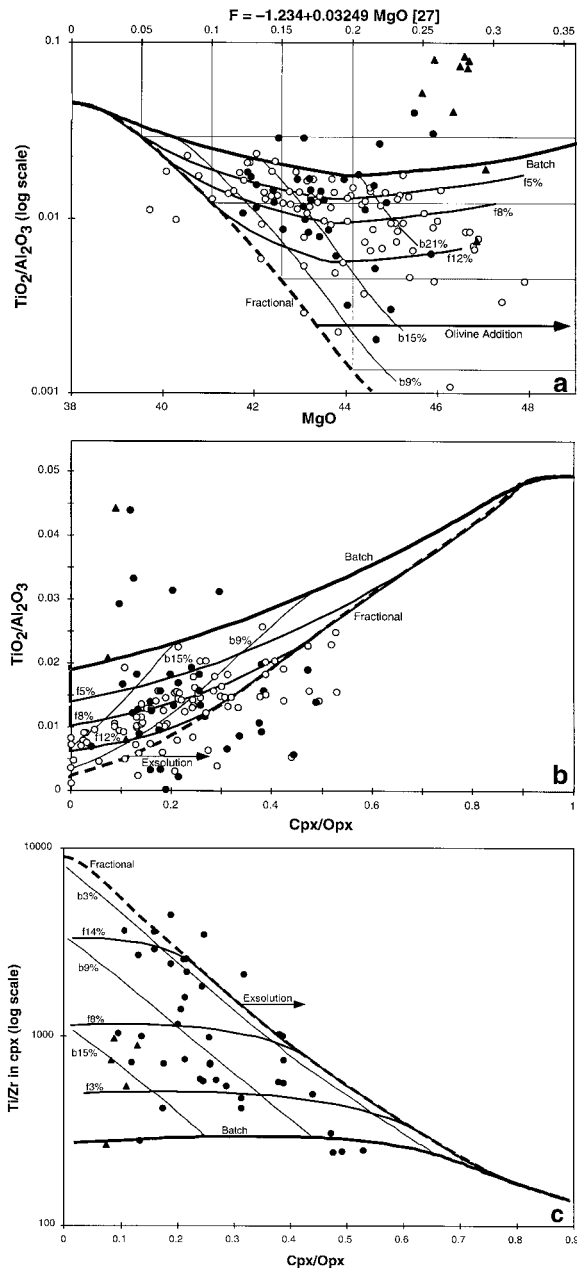


Fig. 6. (a) $\text{TiO}_2/\text{Al}_2\text{O}_3$ (log scale) against MgO (bottom scale) for calculated residue and abyssal peridotite data as in Fig. 5. The top scale converts MgO content to extent of melting F using the approximate linear relationship derived by Niu [27]. Assuming negligible TiO_2 and Al_2O_3 in olivine, subtraction of excess olivine moves samples horizontally to the left; addition of olivine to model residues moves them horizontally to the right. If the data are corrected back to the fractional residue curves, the implied extents of melting cluster around 7 to 12% with a total range from 3 to 21% (except for the high-Ti/Al samples from Hess Deep, which do have high reported TiO_2 in olivine and cannot derive from the McDonough and Sun source by any of the processes considered herein if these olivine analyses are taken at face value). Batch, fractional-followed-by-batch, and batch-followed-by-fractional melting paths reproduce the data compositions without removal of excess olivine at melt fractions ranging up to $\sim 30\%$. (b) $\text{TiO}_2/\text{Al}_2\text{O}_3$ (linear scale) against modal mass ratio of cpx to opx. The samples may have been shifted a small distance to the right by subsolidus exsolution of pyroxenes; data that now plot to the left of the model fractional melting curves, however, seem to require some component of batch melting. (c) Ti/Zr ratio in cpx vs. modal mass ratio of cpx to opx; Zr calculated as a trace element using the partition coefficients of [58]; model curves in this panel show paths that intersect the solidus at 2.0 GPa. Note subset of Indian and Atlantic samples with trace-element data indicated by filled circles is different from subset of data with fully-characterized major-element bulk compositions indicated by filled circles in (a) and (b). Neither Ti/Zr nor cpx/opx should normally be affected by olivine addition. Some equilibrium porous flow or batch melting character is required to produce much of the observed data lying to the left of the fractional trend.

tion of the slow-spreading local trend of Klein and Langmuir [22]. Fractional melting models do not provide sufficient range in Fe contents of primary liquids to create local trends by simple mixing, and although the necessary range of liquids is present in batch melting columns, no systematic mixing rule has been proposed that generates both local and global trends by mixing of batch melts. Explanations that call on high-pressure fractionation generally fail to generate the range in $\text{Fe}_{8.0}$ of typically 1 wt.% observed in many regions and fail to account for the correlation of $\text{Na}_{8.0}$ with Sr contents [21]. Reaction between migrating melts and peridotite in the melting regime or in the overlying lithosphere has been invoked to explain local-trend type systematics in off-axis melts [53,54]. I show below the similar result that the coexistence of near-fractional melting and equilibrium porous flow in the axial melting regime can generate trends resembling slow-spreading local systematics in aggregate basalt composition.

Fig. 7 is a cartoon of the melting regime used in calculations that attempt to capture the possible effects of combining batch and fractional melting. For each potential temperature, aggregate melts were calculated assuming a passive flow geometry for polybaric batch melting, fractional melting, and a series of intermediate models with fractional melting occurring in the deeper part of the melting regime followed by batch melting up to the base of the crust. The liquids extracted in the fractional part of the system are transported to the surface with no further interactions with residues, and mixed with the batch liquids from the top of each column. The transition from fractional to batch is moved from the bottom to the top of the melting regime to generate a family of intermediate models. In this type of triangle model, even the batch melts are transported from the boundaries of the melting regime at depth to the surface with no chemical interactions with the residue, so the aggregate liquid is nowhere in equilibrium with residue. More advanced models, that examine melt migration in two dimensions (e.g., [55]), will be needed to evaluate the consequences of various modes of reactive and isolated melt transport rigorously.

Fig. 8 shows predicted aggregate basalt compositions for various potential temperatures using both

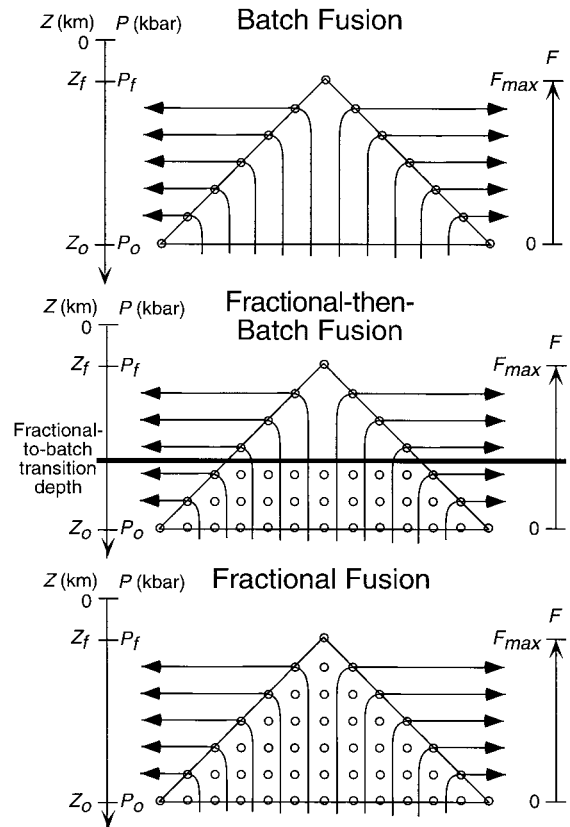


Fig. 7. Cartoon of the calculation used to approximate aggregate liquids from melting regimes that combine aspects of batch and fractional melting. After Langmuir et al. [21], small circles represent points where melt is removed from equilibrium with residue and hence transported to the crust for mixing without further mantle interaction. In a batch melting system, melts are extracted only on the outgoing boundaries of the batch melting regime. In a fractional melting system, melts are extracted at small intervals (an approximation to continuous and instantaneous extraction) throughout the interior of the melting regime as well as on the boundary and brought without further interaction to a site of aggregation. To model an intermediate case, one can perform fractional melting from the solidus up to some transition depth and batch melting from the transition to the base of the crust. Hence melts are extracted throughout the trapezoidal section of the melting regime below the transition, but only from the boundaries of the triangle above the transition. Melts extracted fractionally from the lower trapezoid pass through the upper triangle without chemical interaction. The compositions that result from such a calculation, using two different models of melt production and composition, are shown in Fig. 8.

MELTS and the melting model of Langmuir et al. [21] in melting regimes of the type drawn in Fig. 7. The primary model liquids are fractionated to 8.0

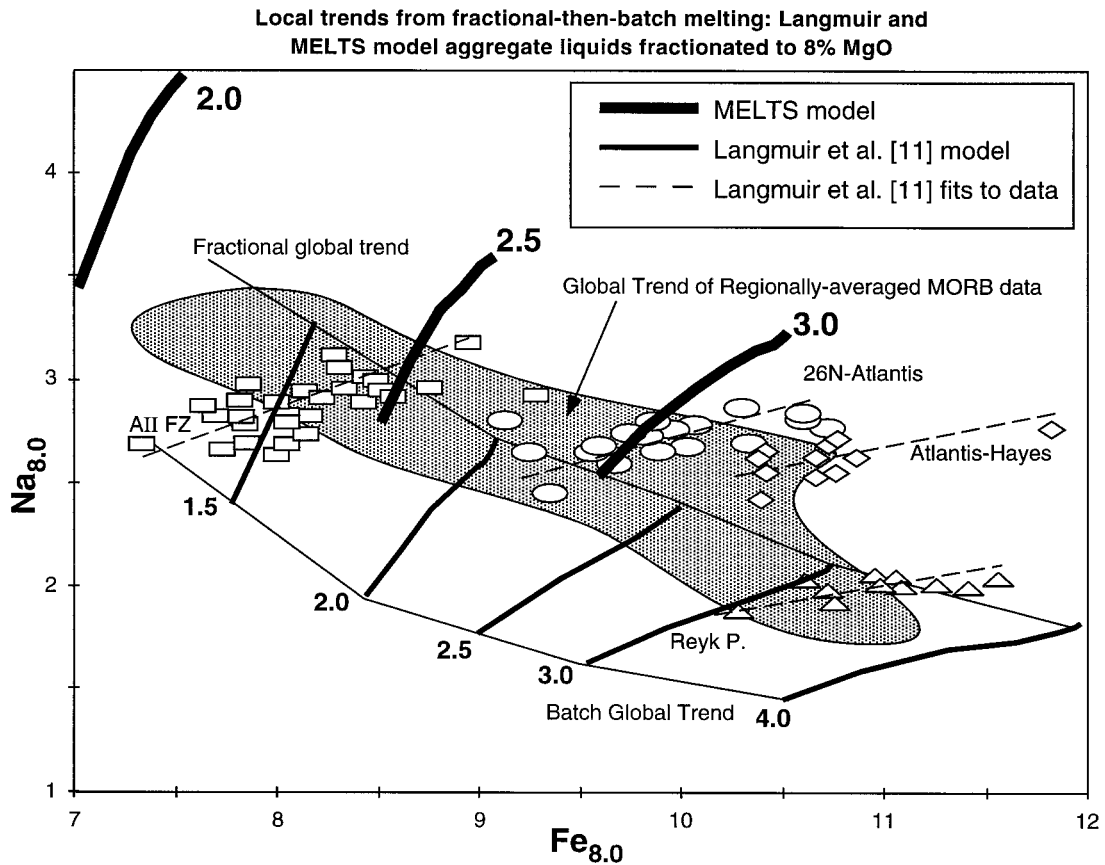


Fig. 8. Basalt compositions resulting from integration of liquids produced by passive flow melting regimes with fractional melting from the solidus up to some pressure followed by batch melting to the base of the crust (see Fig. 7 for a sketch). Source composition from [57]. Primary aggregate liquids calculated by MELTS and by the Langmuir et al. [21] melting model are fractionated to 8.0% MgO using the liquid lines of descent of Langmuir et al. Various curves are labeled by initial pressure of melting; for each potential temperature, the fractional-to-batch transition is varied continuously from the solidus to the base of the crust to generate the heavy curves with positive slopes. Light solid curves connecting the ends of the Langmuir model curves show batch and fractional global trends. Data field shows the global trend of regionally-averaged, fractionation-corrected data and data points with regression lines show selected local trends of unaveraged samples from slow-spreading ridges; data from Langmuir et al. [21].

wt.% MgO using the liquid line of descent slopes from Langmuir et al. [21]; it is difficult to perform a quantitative fractionation correction since the melting model of Langmuir et al. does not predict CaO, Al₂O₃ or H₂O, each of which affects the fractionation path. Hence these calculations would remain approximate even if the melting models were perfect descriptions of the melting process. At given potential temperature, the integrated liquids generated by varying the melting mechanism from all fractional to all batch as the transition sweeps through the melting regime, generate a roughly linear trend in Na–Fe

space with positive slope. Calculations that connect batch to fractional melting by instead continuously varying the residual porosity, by allowing both batch and fractional transport to be present at all levels and varying their proportion, or with batch melting followed by fractional melting, all yield essentially identical curves on this diagram.

The positive slope of the curves linking batch and fractional melting at each potential temperature in Fig. 8 results because:

(1) batch melting is more productive than fractional melting (leading to a higher mean extent of

melting and therefore lower Na in the aggregate liquid);

(2) batch melting leaves more Na behind in the residue at given extent of melting; and

(3) batch melting generates a lower mean pressure of equilibration and hence lower Fe in the aggregate liquid.

The results from MELTS and from the Langmuir et al. model are similar, but MELTS gives about 1% more Na₂O everywhere and falls off toward low extents of melting and low mean pressure of melting (hence high Na_{8,0} and low Fe_{8,0}) more quickly as solidus pressure decreases [33,38]. When the primary liquids from either model are fractionated to 8% MgO they yield a global trend parallel to the data and local trends similar to those for slow-spreading ridges in the high potential temperature range. At low potential temperature, the batch-to-fractional trends at constant potential temperature are clearly steeper than the local trends in the data. The calculation performed is only a first approximation to the range of liquids available in melting regimes that contain elements of fractional fusion and of equilibrium porous flow. The actual partial mixing scenarios that create individual samples along a local trend are undoubtedly more complicated than the perfect two-dimensional integration that produces each point along the model curves in Fig. 8. Nevertheless, these calculations imply that the mixing of increments of liquid generated by the same range of mechanisms required to account for abyssal peridotite compositions at slow spreading ridges may help to explain the local trend systematics in basalt data.

Given the differences in the melt migration history evident in peridotite samples from Hess Deep in the Pacific compared to other ridges, it is notable that the type of local trend that appears to be generated by variable proportions of near-fractional and equilibrium melting is absent in EPR basalts. Langmuir et al. [21] also showed that the regional averages for Pacific ridge segments are systematically offset to lower Na_{8,0} values compared to the Mid-Atlantic Ridge (by about 0.4 wt.%) at given Fe_{8,0}. This is the general effect on average compositions that would be expected if the melting regime at Pacific ridges experienced higher porosity and a more reactive transport character (see Fig. 8 herein and fig. 53 of [21]).

This type of offset, however, is also what would be expected from melting of a more depleted source composition [29,33,56].

4. Conclusions

(1) Although fractional or near-fractional melting alone cannot generate the major-element compositions of abyssal peridotites and batch melting alone cannot generate their trace-element signatures, both major and trace elements in abyssal peridotites are consistent with combined histories of batch and fractional melting, which may be a simple but adequate means to calculate the products of melting regimes that experience variations in the local melt flux, and the extent of re-equilibration during melt migration. It is difficult at present to distinguish, based on major elements or stable trace elements, where in the melting regime each character is dominant.

(2) Variation in the relative contribution of liquids extracted from the melting regime by near-fractional processes and by equilibrium porous flow generates trends similar to the slow-spreading local trend of fractionation corrected basalt compositions, at least for low-Na, high-Fe ridge segments.

(3) Both the local trend in basalt and the highly fractionated trace-element pattern in abyssal peridotites are absent at the East Pacific Rise despite the highly depleted character of the Pacific abyssal peridotites, suggesting that the melt migration system functions differently at high melt fluxes or spreading rates.

Acknowledgements

This paper grew out of discussions with Charlie Langmuir, Ro Kinzler, and Marc Spiegelman. Thanks to Charlie Langmuir for the use of his melting software and fractionation calculations. Mike Baker and John Beckett kindly shared a preprint of their abyssal peridotite manuscript and gave permission to discuss their results in advance of publication. The manuscript benefited from constructive reviews by Peter Kelemen and Rodey Batiza. The author is supported by a postdoctoral research fellowship from Lamont–Doherty Earth Observatory. [FA]

References

- [1] N. von Bargen, H.S. Waff, Permeabilities, interfacial areas and curvatures of partially molten systems: results of numerical computations of equilibrium microstructures, *J. Geophys. Res.* 91 (B9) (1986) 9261–9276.
- [2] H.S. Waff, J.R. Bulau, Equilibrium fluid distribution in an ultramafic partial melt under hydrostatic stress conditions, *J. Geophys. Res.* 84 (1979) 6109–6114.
- [3] D.P. McKenzie, The generation and compaction of partial melts, *J. Petrol.* 25 (1984) 713–765.
- [4] S. Newman, R.C. Finkel, J.D. MacDougall, ^{230}Th – ^{238}U disequilibrium systematics in oceanic tholeiites from 21°N on the East Pacific Rise, *Earth Planet. Sci. Lett.* 65 (1983) 17–33.
- [5] M. Condomines, P. Morand, C.J. Allègre, ^{230}Th – ^{238}U disequilibria in oceanic tholeiites from 21°N on the East Pacific Rise, *Earth Planet. Sci. Lett.* 55 (1981) 393–406.
- [6] D.P. McKenzie, ^{230}Th – ^{238}U disequilibrium and the melting process beneath ridge axes, *Earth Planet. Sci. Lett.* 72 (1985) 149–157.
- [7] P. Beattie, The generation of uranium series disequilibria by partial melting of spinel peridotite: constraints from partitioning studies, *Earth Planet. Sci. Lett.* 117 (1993) 379–391.
- [8] P. Beattie, Uranium–thorium disequilibria and partitioning on melting of garnet peridotite, *Nature* 363 (1993) 63–65.
- [9] H. Iwamori, ^{238}U – ^{230}Th – ^{226}Ra and ^{235}U – ^{231}Pa disequilibria produced by mantle melting with porous and channel flows, *Earth Planet. Sci. Lett.* 125 (1994) 1–16.
- [10] M. Spiegelman, T. Elliott, Consequences of melt transport for uranium series disequilibrium in young lavas, *Earth Planet. Sci. Lett.* 118 (1993) 1–20.
- [11] C.C. Lundstrom, J. Gill, Q. Williams, M.R. Perfit, Mantle melting and basalt extraction by equilibrium porous flow, *Science* 268 (270) (1995) 1958–1961.
- [12] M. Spiegelman, P. Kenyon, The requirements for chemical disequilibrium during magma migration, *Earth Planet. Sci. Lett.* 109 (1992) 611–620.
- [13] S.R. Hart, Equilibration during mantle melting: a fractal tree model, *Proc. Natl. Acad. Sci.* 90 (1993) 11914–11918.
- [14] N.M. Ribe, The generation and composition of partial melts in the earth's mantle, *Earth Planet. Sci. Lett.* 73 (1985) 361–376.
- [15] P.D. Asimow, E.M. Stolper, Steady-state mantle–melt interactions in one dimension: 1. Equilibrium transport and melt focusing, *J. Petrol.* 40 (1999) 475–494.
- [16] P.B. Kelemen, N. Shimizu, V.J.M. Salters, Extraction of mid-ocean-ridge basalt from the mantle by focused flow of melt in dunite channels, *Nature* 375 (1995) 747–753.
- [17] P.B. Kelemen, H.J.B. Dick, Focused melt flow and localized deformation in the upper mantle: juxtaposition of replacive dunite and ductile shear zones in the Josephine peridotite, SW Oregon, *J. Geophys. Res.* 100 (1995) 423–438.
- [18] P.B. Kelemen, Reaction between ultramafic rock and fractionating basaltic magma: I. Phase relations, the origin of calc–alkaline magma series, and the formation of discordant dunite, *J. Petrol.* 31 (1) (1990) 51–98.
- [19] P.B. Kelemen, G. Hirth, N. Shimizu, M. Spiegelman, H.J.B. Dick, A review of melt migration processes in the adiabatically upwelling mantle beneath oceanic spreading ridges, *Philos. Trans. R. Soc. London, Series A* 355 (1997) 283–318.
- [20] P.B. Kelemen, H.J.B. Dick, J.E. Quick, Formation of harzburgite by pervasive melt/rock reaction in the upper mantle, *Nature* 358 (1992) 635–641.
- [21] C.H. Langmuir, E.M. Klein, T. Plank, Petrological systematics of mid-ocean ridge basalts: constraints on melt generation beneath ocean ridges, in: Phipps Morgan, J., Blackman, D.K., Sinton, J.M. (Eds.), *Mantle Flow and Melt Generation at Mid-Ocean Ridges*, American Geophysical Union, *Geophys. Monogr.* 71 (1992) 183–280.
- [22] E.M. Klein, C.H. Langmuir, Local versus global variations in ocean ridge basalt composition: a reply, *J. Geophys. Res.* 94 (B4) (1989) 4241–4252.
- [23] K.T.M. Johnson, H.J.B. Dick, Open system melting and temporal and spatial variation of peridotite and basalt at the Atlantis II Fracture Zone, *J. Geophys. Res.* 97 (B6) (1992) 9219–9241.
- [24] K.T.M. Johnson, H.J.B. Dick, N. Shimizu, Melting in the oceanic upper mantle: an ion microprobe study of diopsides in abyssal peridotites, *J. Geophys. Res.* 95 (1990) 2661–2678.
- [25] H.J.B. Dick, Abyssal peridotites, very slow spreading ridges and ocean ridge magmatism, in: Saunders, A.D., Norry, M.J. (Eds.), *Magmatism in the Ocean Basins*, Geological Society, *Geol. Soc. Spec. Publ.* 42 (1989) 71–105.
- [26] Y. Niu, C.H. Langmuir, R.J. Kinzler, The origin of abyssal peridotites: a new perspective, *Earth Planet. Sci. Lett.* 152 (1997) 251–265.
- [27] Y. Niu, Mantle melting and melt extraction processes beneath ocean ridges: Evidence from abyssal peridotites, *J. Petrol.* 38 (8) (1997) 1047–1074.
- [28] M.B. Baker, J.R. Beckett, The origin of abyssal peridotites: a reinterpretation of constraints based on primary bulk compositions, *Earth Planet. Sci. Lett.*, 1999, in press.
- [29] H.J.B. Dick, J.H. Natland, Late-stage melt evolution and transport in the shallow mantle beneath the East Pacific Rise, in: Mével, C., Gillis, K.M., Allan, J.F., Meyer, P.S. (Eds.), *Proc. Ocean Drill. Program, Sci. Res.* 147, pp. 103–134, Ocean Drilling Program, College Station, TX, 1996.
- [30] Y. Niu, R. Batiza, An empirical method for calculating melt compositions produced beneath mid-ocean ridges: application to axis and off-axis (seamounts) melting, *J. Geophys. Res.* 96 (1991) 21753–21777.
- [31] R.J. Kinzler, Melting of mantle peridotite at pressures approaching the spinel to garnet transition: application to mid-ocean ridge basalt petrogenesis, *J. Geophys. Res.* 102 (B1) (1997) 853–874.
- [32] M.S. Ghiorso, R.O. Sack, Chemical mass transfer in magmatic processes, IV. A revised and internally consistent thermodynamic model for the interpolation and extrapolation of liquid–solid equilibria in magmatic systems at ele-

- vated temperatures and pressures, *Contrib. Mineral. Petrol.* 119 (1995) 197–212.
- [33] P.D. Asimow, A thermodynamic model of adiabatic melting of the mantle, Ph.D. thesis, California Institute of Technology, 1997.
- [34] P.D. Asimow, M.M. Hirschmann, E.M. Stolper, An analysis of variations in isentropic melt productivity, *Philos. Trans. R. Soc. London, Series A* 355 (1997) 255–281.
- [35] P.D. Asimow, M.M. Hirschmann, M.S. Ghiorso, M.J. O'Hara, E.M. Stolper, The effect of pressure-induced solid–solid phase transitions on decompression melting of the mantle, *Geochim. Cosmochim. Acta* 59 (1995) 4489–4506.
- [36] D. Elthon, Chemical trends in abyssal peridotites: refertilization of depleted suboceanic mantle, *J. Geophys. Res.* 97 (B6) (1992) 9015–9025.
- [37] M.B. Baker, M.M. Hirschmann, M.S. Ghiorso, E.M. Stolper, Compositions of low-degree partial melts of peridotite: results from experiments and thermodynamic calculations, *Nature* 375 (6529) (1995) 308–311.
- [38] M.M. Hirschmann, M.S. Ghiorso, L.E. Wasylenki, P.D. Asimow, E.M. Stolper, Calculation of peridotite partial melting from thermodynamic models of minerals and melts, I. Review of methods and comparison to experiments, *J. Petrol.* 39 (6) (1998) 1091–1115.
- [39] M. Constantin, R. Hékinian, D. Ackermann, P. Stoffers, Mafic and ultramafic intrusions into upper mantle peridotites from fast spreading centers of the Easter Microplate (South East Pacific), in: Vissers, R.L.M., Nicolas, A. (Eds.), *Mantle and Lower Crust Exposed in Oceanic Ridges and in Ophiolites*, Kluwer, Dordrecht, 1995, pp. 71–120.
- [40] H.J.B. Dick, R.L. Fisher, W.B. Bryan, Mineralogic variability of the uppermost mantle along mid-ocean ridges, *Earth Planet. Sci. Lett.* 69 (1984) 88–106.
- [41] M. Seyler, E. Bonatti, Regional-scale melt–rock interaction in Iherzolitic mantle in the Romanche Fracture Zone (Atlantic Ocean), *Earth Planet. Sci. Lett.* 146 (1997) 273–287.
- [42] P.J. Michael, E. Bonatti, Petrology of ultramafic rocks from sites 556, 558, and 560 in the North Atlantic, *Init. Rep. Deep Sea Drill. Project* 82 (1985) 523–528.
- [43] P.R. Hamlyn, E. Bonatti, Petrology of mantle-derived ultramafics from the Owen Fracture Zone, Northwest Indian Ocean: Implications for the nature of the oceanic upper mantle, *Earth Planet. Sci. Lett.* 48 (1980) 65–79.
- [44] E.M. Klein, C.H. Langmuir, Global correlations of ocean ridge basalt chemistry with axial depth and crustal thickness, *J. Geophys. Res.* 92 (1987) 8089–8115.
- [45] P.J. Michael, W.C. Cornell, Influence of spreading rate and magma supply on crystallization and assimilation beneath mid-ocean ridges: evidence from chlorine and major element chemistry of mid-ocean ridge basalts, *J. Geophys. Res.* 103 (B8) (1998) 18325–18356.
- [46] M.J. O'Hara, Primary magmas and the origin of basalts, *Scott. J. Geol.* 1 (1965) 19–40.
- [47] E. Aharonov, J.A. Whitehead, P.B. Kelemen, M. Spiegelman, Channeling instability of upwelling melt in the mantle, *J. Geophys. Res.* 100 (B10) (1995) 20433–20450.
- [48] N.H. Sleep, Tapping of melt by veins and dikes, *J. Geophys. Res.* 93 (1988) 10255–10272.
- [49] D.J. Stevenson, Spontaneous small-scale melt segregation in partial melts undergoing deformation, *Geophys. Res. Lett.* 16 (9) (1989) 1067–1070.
- [50] T. Plank, C.H. Langmuir, Effects of the melting regime on the composition of oceanic crust, *J. Geophys. Res.* 97 (B13) (1992) 19749–19770.
- [51] M.J. Daines, D.L. Kohlstedt, The transition from porous to channelized flow due to melt/rock reaction during melt migration, *Geophys. Res. Lett.* 21 (1994) 145–148.
- [52] P.D. Asimow, M.S. Ghiorso, Algorithmic modifications extending MELTS to calculate subsolidus phase relations, *Am. Mineral.* 83 (1998) 1127–1132.
- [53] G.A. Gaetani, S.E. DeLong, D.A. Wark, Petrogenesis of basalts from the Blanco Trough, northeast Pacific: inferences for off-axis melt generation, *J. Geophys. Res.* 100 (1995) 4197–4214.
- [54] Y. Niu, R. Batiza, Chemical variation trends at fast and slow spreading mid-ocean ridges, *J. Geophys. Res.* 98 (1993) 7887–7902.
- [55] M. Spiegelman, Geochemical consequences of melt transport in 2-D: the sensitivity of trace elements to mantle dynamics, *Earth Planet. Sci. Lett.* 139 (1996) 115–132.
- [56] M.M. Hirschmann, M.S. Ghiorso, E.M. Stolper, Calculation of peridotite partial melting from thermodynamic models of minerals and melts, II. Isobaric variations in melts near the solidus and owing to variable source composition, *J. Petrol.* 40 (2) (1999) 297–313.
- [57] W.F. McDonough, S.-s. Sun, The composition of the Earth, *Chem. Geol.* 120 (1995) 223–253.
- [58] D.P. McKenzie, R.K. O'Nions, The source regions of ocean island basalts, *J. Petrol.* 36 (1995) 133–159.